Origin of large thermopower in $LiRh_2O_4$: Calculation of the Seebeck coefficient by the combination of local density approximation and dynamical mean-field theory

R. Arita,[1,*] K. Kuroki,[2] K. Held,[3] A. V. Lukoyanov,[4] S. Skornyakov,[5] and V. I. Anisimov[5]
[1]*RIKEN (The Institute of Physical and Chemical Research), Wako, Saitama 351-0198, Japan*
[2]*University of Electro-Communications, 1-5-1 Chofugaoka, Chofu-shi Tokyo 182-8585, Japan*
[3]*Institute for Solid State Physics, Vienna University of Technology, 1040 Vienna, Austria*
[4]*Ural State Technical University–UPI, 620002 Yekaterinburg, Russia*
[5]*Institute of Metal Physics, Russian Academy of Science–Ural division, 620219 Yekaterinburg, Russia*
(Received 3 June 2008; revised manuscript received 25 August 2008; published 30 September 2008)

Motivated by the newly synthesized mixed-valent spinel $LiRh_2O_4$ for which a large thermopower is observed in the metallic cubic phase above 230 K [Y. Okamoto *et al.*, Phys. Rev. Lett. **101**, 086404 (2008)], we calculate the Seebeck coefficient by the combination of local density approximation and dynamical mean-field theory (LDA+DMFT). The experimental values are well reproduced not only by LDA+DMFT but also by the less involved Boltzmann equation approach. A careful analysis of the latter shows unexpectedly that the origin of the large thermopower shares a common root with a very different oxide: Na_xCoO_2. We also discuss how it is possible to further increase the power factor of $LiRh_2O_4$ through doping, which makes the material even more promising for technological applications.

DOI: 10.1103/PhysRevB.78.115121 PACS number(s): 71.15.−m, 72.15.Jf

I. INTRODUCTION

Designing and searching for good thermoelectric materials have a long history of extensive studies due to the scientific interest and potential technological importance, particularly for generating electrical power from heat (gradients) and for cooling through the Peltier effect.[1] Hitherto, the main target materials have been various insulators or semiconductors such as Bi_2Te_3 (Ref. 1) and $FeSb_2$,[2] since it was believed that huge thermopowers cannot be expected for metals. However, recently, novel metallic systems with large thermopower have been discovered and attracted much attention. Generally, materials with strong electronic correlations are promising;[3] and a famous example is Na_xCoO_2, for which a metallic resistivity as low as $\rho=0.2$ mΩ cm and a thermopower as large as $S=100$ μV/K are observed simultaneously at 300 K.[4] The coexistence of low resistivity and large thermopower results in a large power factor (S^2/ρ), which is especially important for device applications.

Most recently, Okamoto *et al.*[5] synthesized a new mixed-valent spinel oxide, $LiRh_2O_4$. This novel oxide shows two structural phase transitions, i.e., the cubic-to-tetragonal transition at 230 K and the tetragonal-to-orthorhombic transition at 170 K. Particularly interesting is however the high-temperature cubic phase: Despite the metallicity, which is reflected in a small resistivity and the existence of a Fermi edge, the thermopower is as large as 80 μV/K at 800 K, which is exceptional for metallic systems.

On the theoretical side, a variety of studies have been performed to understand the mechanism of large thermopowers in metallic systems. Among others, Koshibae *et al.*[6] derived an expression for the Seebeck coefficient of strongly correlated systems in the high-temperature limit. Considering the orbital and spin degrees of freedom of localized electrons, they estimated the thermoelectric power of Na_xCoO_2 to be 150 μV/K.

However, when the temperature (T) is much lower than the energy scale of the bandwidth ($\sim$2 eV), it is expected that the band dispersion of the system also plays a crucial role as has been suggested from first-principles (band structure) studies.[7,8] Indeed, recently, two of the present authors proposed that the peculiar shape of the valence band (the so-called a_{1g} band) is important to realize a large thermopower and high conductivity in Na_xCoO_2.[9] The different theoretical proposals led to a heated discussion[10] and also to a proposal to discriminate between them through the respective temperature dependence.[11]

The motivation of the present study is to clarify the origin of the large thermopower in $LiRh_2O_4$. For this purpose, we first perform a LDA+DMFT (Ref. 12) calculation (the combination of the local density approximation and the dynamical mean-field theory[13]), employing the Kubo formula for the Seebeck coefficient.[14] This *ab initio* approach is going way beyond Ref. 9, where several phenomenological parameters had to be introduced. Second, we study whether the Boltzmann equation approach with the local density approximation (LDA) band dispersion as an input works well for this system. We will show that this approach gives results quantitatively similar to those of LDA+DMFT. Even though $LiRh_2O_4$ is a material very different from Na_xCoO_2, having among others a much more complicated band structure, our analysis nonetheless reveals that the origin of the large thermopower is similar: the "pudding-mold" shape of the bands crossing the Fermi energy. This outcome was not prejudiced in our investigation and is quite surprising. We also discuss how electron doping could further increase the power factor of $LiRh_2O_4$.

II. METHOD

As a first step we do a LDA calculation for $LiRh_2O_4$, using the linearized muffin tin orbital (LMTO) basis set,[15] employing the experimental lattice constant $a=8.46$ and so-called x parameter $x=0.261$ (which indicates the position of the oxygen sites).

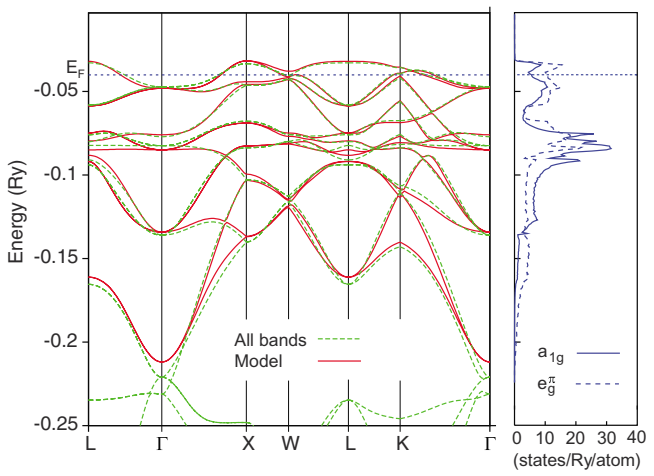

FIG. 1. (Color online) Left panel: Band dispersion of the effective three-orbital Hamiltonian (solid line) and total LMTO band structure (dashed line) of $LiRh_2O_4$. Right panel: partial a_{1g} and e_g^{π} density of states for the model.

From the LMTO band structure, we construct an effective Hamiltonian ($\equiv H_{\alpha\beta}^{\mathrm{LDA}}$) by the projection onto Wannier functions.[16] Since the unit cell of $LiRh_2O_4$ contains four Rh atoms and each Rh atom has three t_{2g} orbitals, the size of the effective Hamiltonian is 12×12. A comparison of the band dispersion of this effective Hamiltonian with the total LDA band structure is shown in Fig. 1. In contrast to the case of Na_xCoO_2,[9] not only the a_{1g} orbital but also the e_g^{π} orbitals have a substantial density of states (see the right panel of Fig. 1) at the Fermi level (E_F). Hence, we cannot extract a simpler effective Hamiltonian from the 12×12 Hamiltonian and need to keep all t_{2g} orbitals in the following calculation.

Next, we supplement the three-orbital Hamiltonian by local intraorbital (U) and interorbital (U') Coulomb repulsions, as well as by Hund's exchange (J of Ising type), and solve it by dynamical mean-field theory (DMFT),[13] using the quantum Monte Carlo (QMC) method. To get high-quality QMC data, we take $\sim 3.0\times 10^7$ sweeps in the calculation.

In the framework of DMFT, the Kubo formula for the Seebeck coefficient is[14]

$$S = \frac{k_B}{e}\frac{A_1}{A_0}, \tag{1}$$

where k_B and e are the Boltzmann constant and unit charge, respectively, and

$$A_n = 2\pi\hbar \int_{-\infty}^{\infty} d\omega \phi^{xx}(\omega) f(\omega) f(-\omega)(\beta\omega)^n, \tag{2}$$

$$\phi^{xx}(\omega) = \frac{1}{V}\sum_{\mathbf{k}} \mathrm{Tr}[v^x(\mathbf{k})\rho(\mathbf{k},\omega)v^x(\mathbf{k})\rho(\mathbf{k},\omega)]. \tag{3}$$

Here, $\rho(\mathbf{k},\omega)$ is the spectral function, i.e., the imaginary part of the Green function $G(\mathbf{k},\omega)$; $v_{\alpha\beta}(\mathbf{k}) \equiv \langle k\beta|(1/m)\nabla_x|k\alpha\rangle$ is the group velocity, $f(\omega)$ the Fermi-Dirac distribution function, and V the volume of the unit cell.

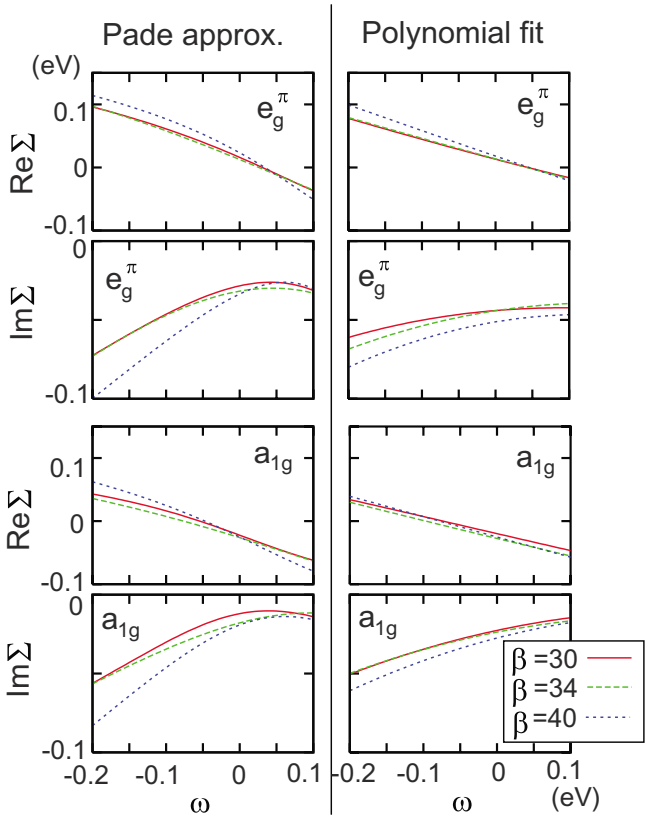

FIG. 2. (Color online) LDA+DMFT(QMC) self-energy calculated by the Pade approximation (left) and a polynomial fit (right).

As is carefully discussed in Ref. 17, when the tight-binding basis is well localized in the real space, we can use the so-called Peirls approximation, $v_{\alpha\beta}(\mathbf{k}) = \nabla_{\mathbf{k}} H_{\alpha\beta}^{\mathrm{LDA}}(\mathbf{k})$.[14] In this method, since we have an analytical expression of $H_{\alpha\beta}^{\mathrm{LDA}}(\mathbf{k})$, the mesh for the momentum sum in Eq. (3) can be arbitrarily dense. In most cases we took a $40\times 40\times 40$ mesh, but in some cases also a $80\times 80\times 80$ mesh for checking convergence.

Usually, $G(\mathbf{k},\omega)$ is calculated in DMFT (QMC) from the self-energy $\Sigma(\omega)$, which is obtained as a root from the local Green function $G^{\mathrm{imp}}(\omega)$, obtained in turn from the QMC data by the maximum entropy method (see, e.g., Refs. 18 and 19). However, this standard approach does not work well for the calculation of the Seebeck coefficient because of the following: Since $\phi^{xx}(\omega)$ only contributes to A_m for $|\omega| \le k_B T$, we need $\Sigma(\omega)$ for small $|\omega|$. For such frequencies $\Sigma(\omega)$ is quite small (smaller than 0.1eV for $|\omega| \le k_B T$, see below). As is pointed out in Ref. 14, this smallness makes it difficult to calculate $\Sigma(\omega)$ reliably especially by a probability-based algorithms such as the maximum entropy method.

Hence, in the present study, we calculate $\Sigma(\omega)$ directly from $\Sigma(i\omega)$, using both the Pade approximation and a polynomial fit. For the former, we apply the algorithm proposed in Ref. 20 to the data with $i\omega \in [0, 45i]$ eV. For the latter, we fit $\Sigma(i\omega)$ for $i\omega \in [0, 4i]$ eV to $\Sigma_{n=0}^{5} c_n (i\omega)^n$ by a standard least-squares fit. Since only the behavior at small $|\omega|$ is relevant for the Seebeck coefficient, we can expect the polynomial fit to give reasonable results. The Pade approximation might become problematic if poles are present in the vicinity

of the real-ω axis. However, as we will see below, the resulting $\Sigma(\omega)$ for the present case does not show any anomalous behavior for small $|\omega|$, which implies that the Pade approximation is not problematic.

In Fig. 2, we plot $\Sigma(\omega)$ for $(U,U',J)=(3.1,1.7,0.7)$ eV, which was estimated in Ref. 18 and $\beta=1/k_BT=30,34,40$ eV^{-1}. For $T\sim 300$ K, the main contribution stems from $\omega\in[-0.03,0.03]$ eV. For these energies Pade approximation and polynomial fit give similar results. Even though the agreement is not perfect, differences are small, i.e., of $O(0.01)$ eV. Thus we employ $\Sigma(\omega)$ of both Pade approximation and polynomial fitting in the following LDA+DMFT calculation of the Seebeck coefficient. The difference gives us an estimate for the accuracy of our calculation.

Besides the LDA+DMFT study, we also performed calculations based on the Boltzmann equation. The Seebeck coefficient can be estimated by calculating

$$S=\frac{1}{eT}\frac{K_1}{K_0}, \tag{4}$$

$$K_n=\sum_{\mathbf{k},\alpha}\tau u_\alpha(\mathbf{k})u_\alpha(\mathbf{k})\left(-\frac{\partial f(\epsilon)}{\partial\epsilon}\right)_{\epsilon=\epsilon(\mathbf{k})_\alpha}\epsilon(\mathbf{k})_\alpha^n. \tag{5}$$

Here, τ is the relaxation time which we assume to be independent of $\mathbf{k}$; $\epsilon_\alpha(\mathbf{k})$ are the eigenvalues of $H^{\mathrm{LDA}}_{\alpha,\beta}(\mathbf{k})$; and $u_\alpha(\mathbf{k})$ the diagonal elements of $\tilde{U}^\dagger v_{\alpha,\beta}(\mathbf{k})\tilde{U}$, where $\tilde{U}$ is the unitary transformation which diagonalizes $H^{\mathrm{LDA}}_{\alpha\beta}(\mathbf{k})$.

Note that K_n can be roughly estimated as

$$K_0\sim\tilde{\sum}(u_A^2+u_B^2), \tag{6}$$

$$K_1\sim(k_BT)\tilde{\sum}(u_B^2-u_A^2), \tag{7}$$

apart from a constant factor.[9] Here, $\tilde{\Sigma}$ is a summation over the states in the range of $|\epsilon(k)|<O(k_BT)$, and u_A and u_B are typical velocities for the states below and above the Fermi level, respectively.

III. RESULTS

In Fig. 3, we show the resulting Seebeck coefficient calculated by the LDA+DMFT method and the Boltzmann equation approach. We also plot the result of the constant-τ approximation for the Kubo formula, i.e., we assume $\Sigma(\omega)=-1.0^{-3}i$ for Eqs. (1)–(3).

From Fig. 3, we see that (1) the Boltzmann equation and the constant-τ approximation for the Kubo formula give almost the same result; (2) the constant-τ approximation gives a larger thermopower than LDA+DMFT; and (3) this smaller LDA+DMFT thermopower is closer to experiment,[5] already for $(U,U',J)=(3.1,1.7,0.7)$ eV (Ref. 18) but even more so for somewhat smaller values of the Coulomb interaction.

Point (1) demonstrates that the calculation via Eq. (1) is working well, if $\Sigma(\omega)$ is correct. Point (2) can be understood from the behavior of $-\mathrm{Im}\,\Sigma(\omega)$: Fig. 2 shows that $-\mathrm{Im}\,\Sigma(\omega)$ calculated by the LDA+DMFT method is large for negative

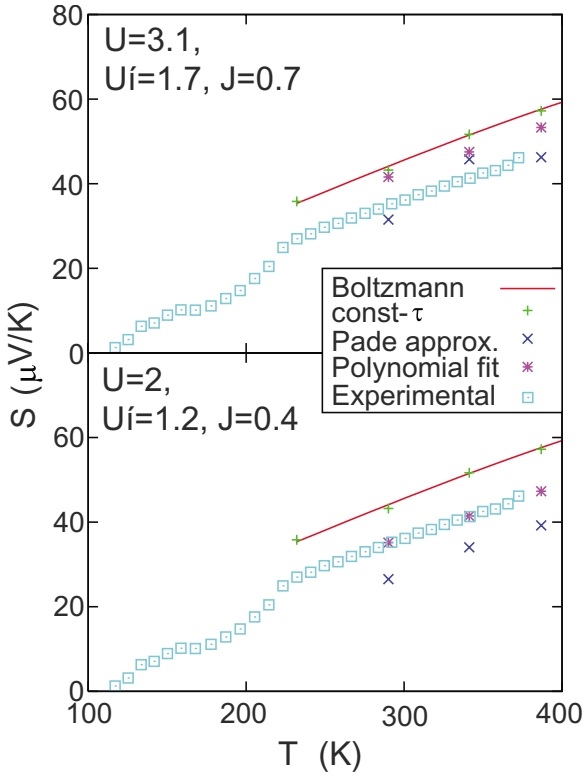

FIG. 3. (Color online) Thermopower calculated by the Boltzmann equation approach and the constant-τ method, as well as by LDA+DMFT, using both the Pade approximation and a polynomial fit for the self-energy.

ω but small for positive ω (independently of Pade approximation and polynomial fit). This means that, in contrast to the constant-τ approximation, the actual life time of quasiholes is longer than that for quasiparticles. Therefore, the contribution of the quasiholes (particles) to ϕ^{xx} in Eq. (1) becomes larger (smaller) in the LDA+DMFT calculation, and consequently the first moment, A_1, becomes smaller. Here, it should be noted that the constant-τ approximation does not correspond to the limit of $U=U'=J=0$, since this asymmetry of life time exists even in the weak coupling limit. This is the reason why the results of LDA+DMFT move away from those of the constant-τ approximation as U, U', and J are decreased.

As for point (3), we would like to note that the correlations renormalize the bandwidth. This renormalization is calculated microscopically here whereas it has been adjusted to the angle-resolved photoemission spectrum in Ref. 9.

IV. DISCUSSION

While there are some differences between Boltzmann equation approach and LDA+DMFT, the results are still very similar, even *quantitatively*. Hence, we may expect that, in the present case, the Boltzmann equation can be used as a convenient tool to analyze the mechanism of the large thermopower, or even to design more efficient thermoelectric materials.

Let us first examine whether the mechanism proposed for Na_xCoO_2 in Ref. 9 can work also in $LiRh_2O_4$. If the valence

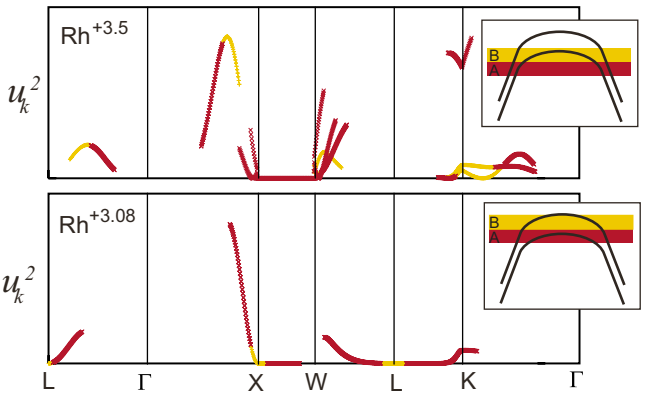

FIG. 4. (Color online) Group velocity squared (u_k^2) along different directions of the first Brillouin zone for $Rh^{+3.5}$ ($LiRh_2O_4$; upper panel) and $Rh^{+3.08}$ (electron-doped $LiRh_2O_4$; lower panel). k points above the Fermi energy E_F are shown in yellow (light gray), those below E_F in red (dark gray).

band has a peculiar shape of dispersion which is dispersive below the E_F but somewhat flat above (the so-called "pudding-mold" type), K_1 in Eq. (7) becomes large, since the group velocity above E_F (u_A^2) is much larger than the one below E_F (u_B^2) in this case. This is the basic idea of Ref. 9 of how to realize a large thermopower and a low resistivity at the same time.[21] In the top panel of Fig. 4, we plot the group velocity squared for $LiRh_2O_4$ within the energy window of $|\varepsilon - E_F| < 3k_BT$ at $T \simeq 300$ K. We see that u_A^2 is indeed larger than u_B^2, confirming this mechanism. We note here that although the Rh valence is +3.5 in $LiRh_2O_4$, the degeneracy of d_{xy}, d_{yz}, and d_{zx} orbitals in the cubic phase makes the number of holes *per band* small, resulting in a situation similar to Na_xCoO_2 with the Co valence smaller than +3.5. This view is consistent with the experimental fact that the thermopower is suppressed in the tetragonal phase below 230 K, where the degeneracy is lifted.[5]

However, we also see that the (squared) group velocity above E_F is still large for some k points. In fact, for $LiRh_2O_4$, there are two pudding-mold bands. For the Rh valence of +3.5, E_F lies near the bending point of one of the pudding-mold bands, but also cuts through the dispersive portion of the other (see the upper inset of Fig. 4). The former enhances the thermopower, while the latter suppresses it. This might be the reason why $LiRh_2O_4$ is not such a good thermoelectric material as Na_xCoO_2.

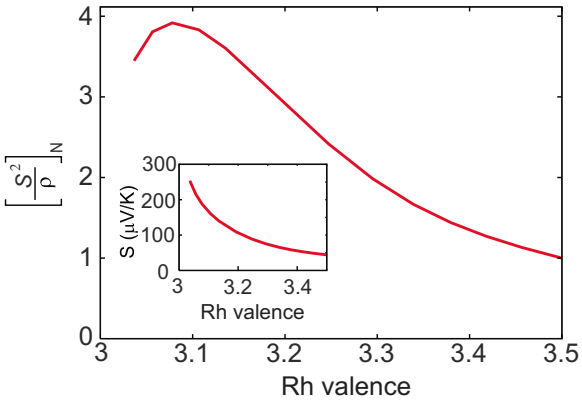

FIG. 5. (Color online) Power factor (normalized by its value at Rh valence = +3.5) and thermopower (inset) as a function of the valence of Rh, calculated by the Boltzmann equation.

To enhance the thermopower in $LiRh_2O_4$, we suggest the following possibility: If we dope electrons to this system, one of the pudding-mold bands will be brought completely below E_F (see the lower inset of Fig. 4). The second panel of Fig. 4 shows the group velocity squared for such a doped system with Rh valence +3.08. In this case, the group velocity squared above E_F is small for the entire Brillouin zone.

To confirm this idea, we calculate the thermopower and the power factor (normalized by its value at Rh valence = +3.5) for various Rh valences by means of the Boltzmann equation approach[22] (see Fig. 5). The results indicate a maximal power factor ($=S^2/\rho \propto K_1^2/K_0^3$) at a valency of +3.08, where it is almost four times larger than for $LiRh_2O_4$. While the orbital degeneracy of d_{xy}, d_{yz}, and d_{zx} already plays a crucial role to make E_F be higher than those of single-orbital systems,[5] realizing this situation experimentally is an interesting challenge which seems to be feasible.

ACKNOWLEDGMENTS

We would like to thank H. Takagi and Y. Okamoto for fruitful discussions and for providing the experimental data shown in Fig. 3. Numerical calculations were performed at the facilities of the Supercomputer center, ISSP, University of Tokyo. This work was supported by Grants-in-Aid for Scientific Research (MEXT, Japan) Grants No. 19019012, No. 19014022, and No. 19051016 and Russian Foundation for Basic Research (RFBR) Grant No. 07-02-00041.

*Present address: Department of Applied Physics, University of Tokyo, Tokyo 113-8656, Japan.

[1] G. D. Mahan, Solid State Phys. **51**, 81 (1997); G. D. Mahan, B. Sales, and J. Sharp, Phys. Today **50** (3), 42 (1997)

[2] A. Bentien, S. Johnsen, G. K. H. Madsen, B. B. Iversen, and F. Steglich, Europhys. Lett. **80**, 39901 (2007).

[3] S. Paschen, *CRC Handbook of Thermoelectrics*, edited by D. M. Rowe (CRC, Boca Raton, FL, 2005), Chap. 15; A. Bentien, S. Johnsen, G. K. H. Madsen, B. B. Iversen, and F. Steglich, Europhys. Lett. **80**, 17008 (2007).

[4] I. Terasaki, Y. Sasago, and K. Uchinokura, Phys. Rev. B **56**, R12685 (1997).

[5] Y. Okamoto, S. Niitaka, M. Uchida, T. Waki, M. Takigawa, Y. Nakatsu, A. Sekiyama, S. Suga, R. Arita, and H. Takagi, Phys. Rev. Lett. **101**, 086404 (2008).

[6] W. Koshibae, K. Tsutsui, and S. Maekawa, Phys. Rev. B **62**, 6869 (2000).

[7] D. J. Singh, Phys. Rev. B **61**, 13397 (2000).

[8] G. B. Wilson-Short, D. J. Singh, M. Fornari, and M. Suewattana, Phys. Rev. B **75**, 035121 (2007).
[9] K. Kuroki and R. Arita, J. Phys. Soc. Jpn. **76**, 083707 (2007).
[10] I. Terasaki, JPSJ Online-News and Comments [Oct. **10**, 2007].
[11] Y. Ishida, H. Ohta, A. Fujimori, and H. Hosono, J. Phys. Soc. Jpn. **76**, 103709 (2007).
[12] V. I. Anisimov, A. I. Poteryaev, M. A. Korotin, A. O. Anokhin, and G. Kotliar, J. Phys.: Condens. Matter **9**, 7359 (1997); A. I. Lichtenstein and M. I. Katsnelson, Phys. Rev. B **57**, 6884 (1998); K. Held, I. A. Nekrasov, G. Keller, V. Eyert, N. Blümer, A. K. McMahan, R. T. Scalettar, Th. Pruschke, V. I. Anisimov, and D. Vollhardt, Phys. Status Solidi B **243**, 2599 (2006); G. Kotliar, S. Y. Savrasov, K. Haule, V. S. Oudovenko, O. Parcollet, and C. A. Marianetti, Rev. Mod. Phys. **78**, 865 (2006); K. Held, Adv. Phys. **56**, 829 (2007).
[13] W. Metzner and D. Vollhardt, Phys. Rev. Lett. **62**, 324 (1989); A. Georges and G. Kotliar, Phys. Rev. B **45**, 6479 (1992); A. Georges, G. Kotliar, W. Krauth, and M. J. Rozenberg, Rev. Mod. Phys. **68**, 13 (1996).
[14] V. S. Oudovenko, G. Palsson, K. Haule, G. Kotliar, and S. Y. Savrasov, Phys. Rev. B **73**, 035120 (2006).
[15] O. K. Andersen, Phys. Rev. B **12**, 3060 (1975); O. Gunnarsson, O. Jepsen, and O. K. Andersen, *ibid.* **27**, 7144 (1983).
[16] V. I. Anisimov, D. E. Kondakov, A. V. Kozhevnikov, I. A. Nekrasov, Z. V. Pchelkina, J. W. Allen, S.-K. Mo, H.-D. Kim, P. Metcalf, S. Suga, A. Sekiyama, G. Keller, I. Leonov, X. Ren, and D. Vollhardt, Phys. Rev. B **71**, 125119 (2005).
[17] I. Paul and G. Kotliar, Phys. Rev. B **67**, 115131 (2003).
[18] Z. V. Pchelkina, I. A. Nekrasov, T. Pruschke, A. Sekiyama, S. Suga, V. I. Anisimov, and D. Vollhardt, Phys. Rev. B **75**, 035122 (2007).
[19] I. A. Nekrasov, K. Held, G. Keller, D. E. Kondakov, T. Pruschke, M. Kollar, O. K. Andersen, V. I. Anisimov, and D. Vollhardt, Phys. Rev. B **73**, 155112 (2006).
[20] H. J. Vidberg and J. W. Serene, J. Low Temp. Phys. **29**, 179 (1977).
[21] Note that this idea is totally different from the conventional idea to realize large thermopower, exploiting an asymmetry of density of states (DOS) around the Fermi level. While DOS roughly scales as $\langle 1/u(\mathbf{k})\rangle$, the quantity which plays crucial role here is $\langle u^2(\mathbf{k})\rangle$. These quantities behave quite differently in general. For example, for the case of Na_xCoO_2, if we calculate the former taking into account the dispersion along the z axis, we see that it has no special structure around the Fermi level. However, on the other hand, the latter has a strong asymmetry, which we believe to be the origin of large thermopower in this material.
[22] Note that this calculation neglects the energy and filling dependence of τ, which should be present and affect ρ and the power factor. Nevertheless, since the effect of the frequency dependence of τ is not so serious in the calculation of the Seebeck coefficient (Fig. 3), we believe that the present estimation of the power factor at least gives the correct tendency of the filling dependence, especially if the Rh valence does not change drastically.